Theoretical Study of $[Na(H_2O)_n]^-$ ($n = 1-4$) Clusters: Geometries, Vertical Detachment Energies, and IR Spectra

Kenro Hashimoto,* Tetsuya Kamimoto, and Kota Daigoku

Computer Center and Department of Chemistry, Tokyo Metropolitan University/ACT-JST, 1-1 Minami-Ohsawa, Hachioji-shi, Tokyo 192-0397, Japan

Received: July 22, 1999; In Final Form: February 9, 2000

Geometries, vertical detachment energies (VDEs), and IR spectra of $[Na(H_2O)_n]^-$ ($n = 1-4$) have been investigated by an ab initio MO method at the correlated level. Water molecules are bound to Na^- via Na−H as well as hydrogen-bond interactions. The calculated VDEs are in good agreement with the recent photoelectron spectroscopy, and all observed bands are assignable to the $3^2S(Na)-3^1S(Na^-)$ and $3^2P(Na)-3^1S(Na^-)$ type transitions perturbed by hydration. They are shifted to higher energy with increasing n by keeping their separation almost unchanged, which reflects the hydration structure of Na^-. We also report the calculated IR spectra that are informative about the ionic Na−H bonds and the hydrogen-bond network among water molecules in the clusters.

1. Introduction

The understanding of solvation phenomena at the molecular level is of fundamental importance in wide areas of chemistry.[1] Clusters containing a single alkali metal atom, and polar solvent molecules are expected to serve as a model for studying the formation, structure, and energetics of a solvated electron and a solvated metal cation and have been actively investigated in recent years.[2−28] Experimental findings of the unusual size dependence of the ionization potentials (IPs) for the $M(H_2O)_n$ and $M(NH_3)_n$ (M = Li,[16] Na[2], and Cs[13]) type clusters have stimulated many theoretical studies about their structures and the localization mode of the excess electron.[19−27] However, since the experimental data were limited to the IP measurement, the new efforts to access the neutral ground and excited states of these clusters have been started.[7−12,14−17]

Takasu et al. have observed the photoelectron spectra (PES) of negatively charged Na atom embedded in water and ammonia clusters very recently.[16] They found the different size dependence of the band positions for $[Na(H_2O)_n]^-$ from that of $[Na(NH_3)_n]^-$. That is, both first and second PES bands of $[Na(H_2O)_n]^-$ ($n \leq 7$) are shifted gradually to higher electron binding energy (EBE) with increasing n by keeping their separation almost unchanged. On the other hand, for $[Na(NH_3)_n]^-$, the vertical detachment energy (VDE) of the first PES band is shifted slightly to lower EBE, while that of the second band decreases dramatically as n grows. In addition, the photoelectron bands of both $[Li(H_2O)_n]^-$ and $[Li(NH_3)_n]^-$ have been found to behave similarly to those of $[Na(NH_3)_n]^-$.

In the previous paper,[28] we have reported our preliminary results on $[M(H_2O)_n]^-$ and $[M(NH_3)_n]^-$ (M = Na and Li, $n = 1-3$) and argued several structures and their VDEs for the first PES band by the coupled cluster method. However, the questions regarding whether the possible isomers are also responsible for the second band and why the PES bands show the characteristic behavior depending on the combinations of alkali metal and solvent have remained unresolved.

* Corresponding author. Fax: +81-426-77-1352. E-mail: hashimoto-kenro@c.metro-u.ac.jp.

In the present work, we have concentrated on the $[Na(H_2O)_n]^-$ whose size dependence of the PES bands is unique among the solvation clusters of alkali metals studied experimentally. We have extended our study for n up to 4 and examined the low-energy isomers extensively. The multireference configuration interaction method has been employed to assign not only the first PES band but also the second one. The size dependence of the VDEs has been analyzed in connection with the electronic nature of the final neutral states at the anionic geometries. We will also report the calculated IR spectra to discuss the vibrational feature of these clusters.

2. Method

The molecular structures of $[Na(H_2O)_n]^-$ ($n = 1-4$) were optimized by using the energy gradient technique for the second-order many-body perturbation method (MP2). Vibrational analysis using the analytical second-derivative matrix was carried out to confirm the minima on the potential energy surfaces. The basis set employed for Na was McLean−Chandler's [12s9p/6s5p] basis set[29] augmented by double d type polarization functions ($\alpha = 0.5$ and 0.15) and a diffuse sp function ($\alpha = 0.0076$). The basis sets for the O and H atoms were the 6-311+G(d,p).[30] To take the zero-point vibrational correction (ZPC) into account in total binding energies, we used scaled harmonic frequencies. The scale factor was obtained from the average ratio of the experimental[31] and calculated harmonic frequencies for an isolated H_2O molecule. We carried out two types of MP2 calculations to estimate the effect of freezing core orbitals on the geometries and energetics. In one method, all **1s** orbitals on heavy atoms were frozen, while we employed the usual frozen core approximation in another.

Vertical detachment energies were calculated by the multi-reference single and double excitation configuration interaction (MRSDCI) method preceded by multiconfiguration self-consistent field (MCSCF) calculation[32−36] at the optimized geometries. Five valence molecular orbitals corresponding to **3s**, **3p**, and **4s** orbitals on Na were included in the active space of the MCSCF calculations. For anions, five configurations in which one of the active orbitals was doubly occupied were

10.1021/jp992525n CCC: $19.00
Published on Web 03/29/2000

considered, and the MCSCF wave function was optimized for the ground state. For the neutrals, five configurations in each of which the unpaired electron occupied one of the five active orbitals were taken into account, and the five low-lying doublet states were averaged with equal weight. The natural orbitals (NOs) obtained by these MCSCF procedures were used as one-particle functions in the MRSDCI calculations where the configurations treated in the MCSCF methods constructed the reference space. We considered all single and double excitations from the above active orbitals on Na as well as 2*n* high-lying orbitals corresponding mainly to lone pair orbitals in water molecules. Radial distribution of the unpaired electron for each neutral state was evaluated by the square root of the sum of the orbital components of the diagonal elements of the second moment for the CI−NO whose occupation number is close to one (>0.99).

The Gaussian series of programs[37] was used for the geometry optimization and the vibrational analysis. The program used for the MCSCF and CI calculations was MOLPRO-96.[38]

3. Results and Discussion

3.1. Geometries and Energetics of $[Na(H_2O)_n]^-$ ($n = 1-4$). The optimized structures of $[Na(H_2O)_n]^-$ ($n = 1-4$) are shown in Figures 1 and 2. We use labels of the form [*i*,*j*,*k*] to classify the structures. The values of the *i* and *j* are the numbers of the water molecules bound to Na^- from the hydrogen side and oxygen side, respectively. The value of the *k* indicates the number of hydrogen bonds among water molecules. Total binding energies (TBEs) including the ZPC by the scaled harmonic frequencies are also given for each structure. In the previous paper, we assessed the basis set superposition error for TBEs by the counter-poise correction (CPC). The decrease of TBEs by CPC depended on the structure, but it was at most a few kilocalories/mole per water molecule, and the structures with Na−H and hydrogen-bond interactions were more stable than those with Na−O bonds with the same *n* even when the CPC was taken into account. The TBE values for the complexes in Figures 1 and 2 are without CPC. Throughout $n = 1-4$, freezing the **2s** and **2p** orbitals of Na in the MP2 calculations results in the lengthening of the distances between Na and O atoms in the water molecules interacting directly with Na^-. However, TBEs calculated with and without correlating the electrons in these low-energy orbitals are very close to each other for all structures examined. Thus, we discuss only the TBEs with all **1s** orbitals of heavy atoms frozen in the following paragraphs.

For $n = 1$, two stable structures have been found. A water molecule is bound to Na^- from the hydrogen side in **1a** and from oxygen side in **1b**. The symmetric geometry of **1a**, whose TBE is 4.9 kcal/mol, is governed by the electrostatic interaction between a negative charge on Na and two positive charges on hydrogens. It is known for the hydrated halogen anions $[X(H_2O)]^-$ (X = F, Cl, Br and I) that a water monomer is also bound by the X^-−H interaction.[39−47] However, they form an asymmetric C_s structure which has been attributed to the polarized OH bond.[42] The X−H−O angle decreases and the two OH lengths become close to each other as the X−H bond distance, namely, the radius of X^-, increases and as the TBE becomes smaller. The symmetric C_{2v} form of **1a** is considered to be in this correlation. In fact, the Na−H distances in **1a** are longer than the I−H length (2.860 Å)[42] and its TBE is less than that of $[I(H_2O)]^-$ (10.3 kcal/mol).[42] On the other hand, the isomer like **1b** is unknown for the halogen anions. In **1b**, not only the **3s** orbital on Na but also the low-lying vacant **3p** orbitals can contribute to the valence MOs. This orbital mixing plays an important role in determining electron distribution and reducing the destabilization of the valence MOs by the complex formation. Actually, the HOMO electron density in **1b** is distributed in the vicinity of Na and extends widely in space in the directions opposite to the water, which is similar to the neutral $Na(H_2O)$[25] and $Li(H_2O)$.[27] TBE for **1b** is less than that of **1a** by ∼1 kcal/mol.

For $n = 2$, we have obtained six minimum structures (**2a**−**2f**). The most stable structures are the [1,0,1] forms (**2a** and **2b**) in which the second water is bound to **1a** via a hydrogen bond with different water orientation. Though we optimized the C_2 symmetric [2,0,2] structure, where each water molecule points one OH to Na^- and donates another OH to a hydrogen-bond network with the other water, it was higher in energy than **2a** by 2.5(3.2) kcal/mol with(without) ZPC and had an imaginary frequency. The further optimization following the normal mode corresponding to the imaginary frequency reached **2a**. These lowest-energy structures **2a** and **2b** can be also regarded as the complexes where a water dimer is bound to Na^-. The binding energy of a water dimer is calculated to be 3.7 kcal/mol, which is in good agreement with the experimental value (3.6 ± 0.5 kcal/mol)[48] and the theoretical values (3.2−3.9 kcal/mol)[49] at the same level with the better basis sets. The water−water interaction energy in **2a** is 4.8 kcal/mol, which is more than 30% of the TBE without ZPC (15.3 kcal/mol). Thus, the hydrogen bonding between water molecules plays an important role in gaining TBE in this type of complex. The second most stable structures are **2c** and **2d**, whose TBEs are ∼10 kcal/mol. The former has an Na−O bond and a hydrogen bond, while the latter has two equivalent Na−O bonds and no hydrogen bond. Other optimized structures (**2e** and **2f**) have [0,1,1] and [1,1,0] forms and they are less stable than **2a** by more than ∼3 kcal/mol.

For $n = 3$, we have optimized eighteen equilibrium structures. The five low-energy isomers are shown in Figure 1 and their TBEs are 20.2−18.1 kcal/mol. Other isomers which are higher in energy than the most stable **3a** by more than ∼3 kcal/mol are given in the Supporting Information (Figure 1S). In the [1,0,2] structure **3a**, the third water molecule is bound to **2a** through hydrogen bond. **3b** is a [2,0,2] type complex in which two water molecules are bound to Na^- from the hydrogen sides and they are bridged by the third water via hydrogen bonds. This isomer is an analogue of the ring structure with C_s symmetry found for $[F(H_2O)_3]^-$ [44] and $[Cl(H_2O)_3]^-$.[46] **3c** and **3e** have the [3,0,3] and [0,3,3] forms, where a cyclic water trimer is bound to Na^-. Each water molecule points one OH bond to Na^- and another OH to an O atom in the neighboring H_2O in the former, while Na^- is bound by water molecules by Na−O bonds in the latter. **3c** is a member of the pyramidal complex found for hydrated halogen anions. On the other hand, **3e** is similar to the most stable neutral $Na(H_2O)_3$.[24] We call this structure the Na−O surface structure, since the pyramidal structure has been sometimes called the surface cluster.[50,51] **3d** is the [1,0,2] complex in which two water molecules are bound equivalently to **1a** via hydrogen bonds. It can be also regarded as the cluster where the third water molecule is bound to **2a** through a hydrogen bond.

As regards $n = 4$, the number of potential minimum configurations is expected to be very large. Since the low-energy $n \leq 3$ complexes tend to have the structure where water clusters are bound to Na^- via Na−H interaction by rearranging the hydrogen bonds among waters, we narrowed our focus mainly to the structure with as many Na−H and hydrogen bonds as

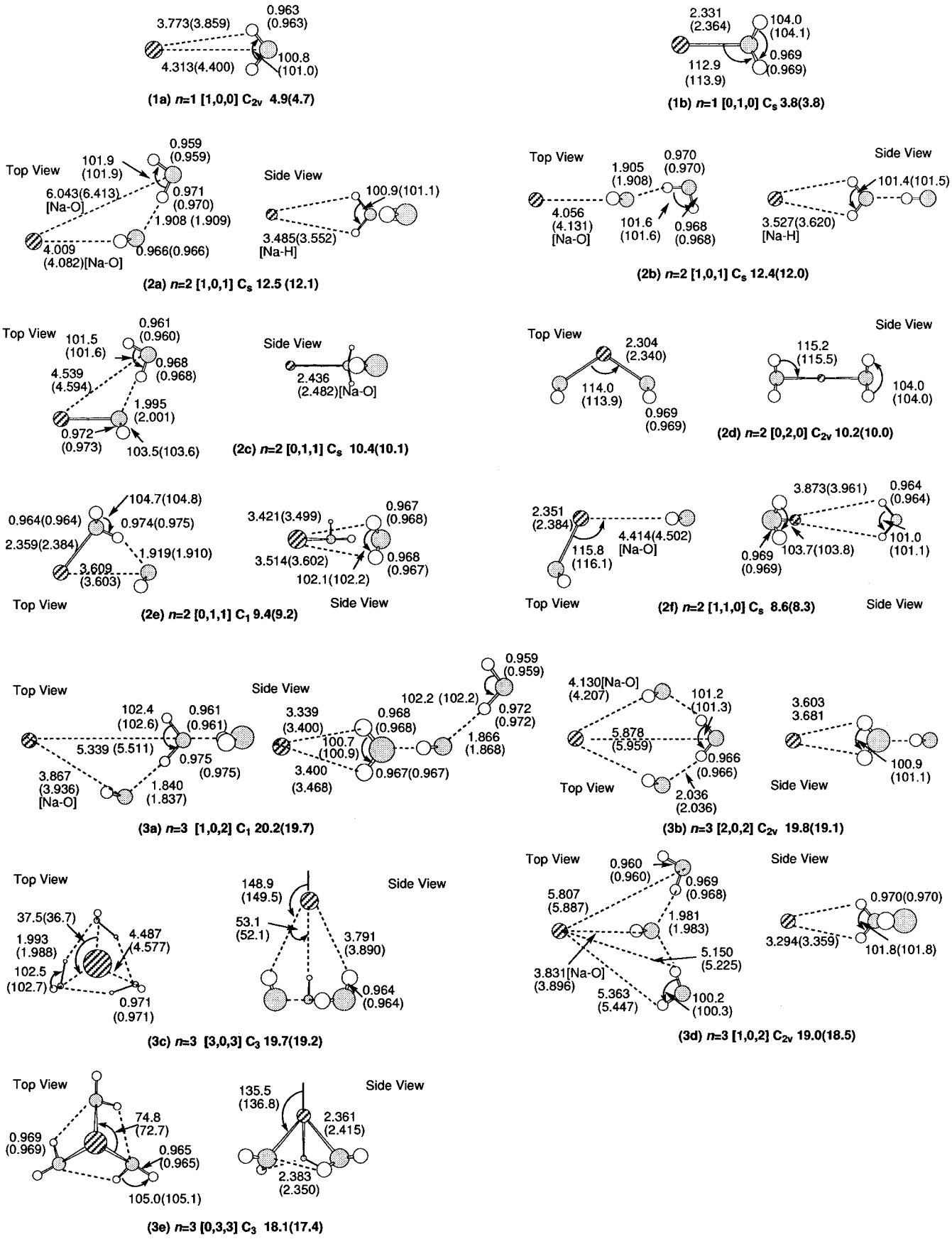

Figure 1. Optimized geometries of $[Na(H_2O)_n]^-$ ($n = 1-3$) at the MP2 level with all **1s** orbital frozen. Geometrical parameters are given in Å and degrees. The molecular symmetry and total binding energies (kcal/mol) with ZPC with the scaled harmonic frequencies are given under each structure. Values in parentheses are with usual frozen core approximation.

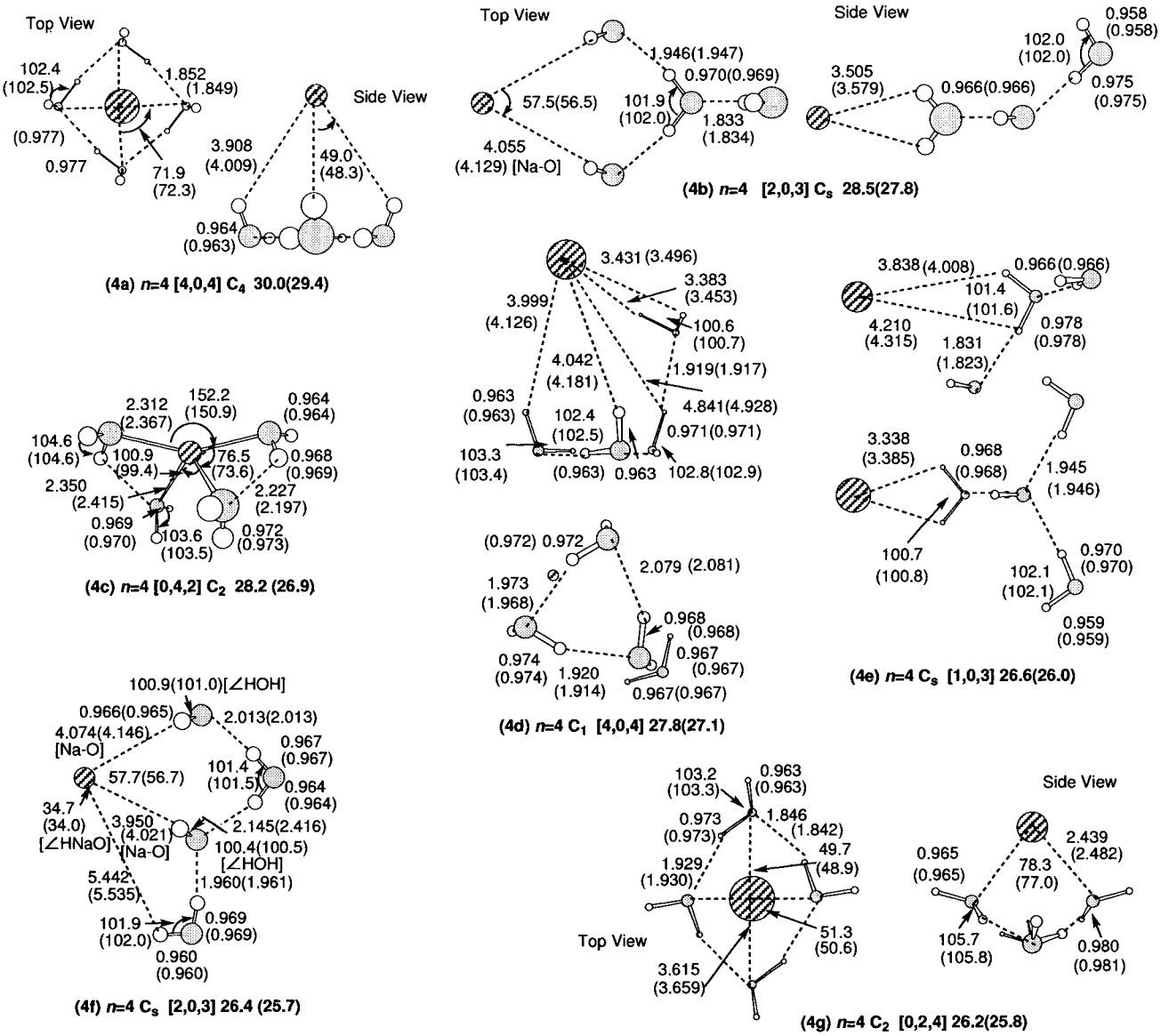

Figure 2. Optimized geometries of $[Na(H_2O)_4]^-$ at the MP2 level with all **1s** orbital frozen. Geometrical parameters are given in Å and degrees. The molecular symmetry and total binding energies (kcal/mol) with ZPC with the scaled harmonic frequencies are given under each structure. Values in parentheses are with usual frozen core approximation.

possible and the isomers in which the fourth water molecule is bound to the low-energy $n = 3$ clusters through hydrogen bonds. **4a** is of [4,0,4] form and a pyramidal complex whose TBE is 30.0 kcal/mol. The isomers **4b**, **4d**, **4e**, and **4f** are the structures where the fourth water monomer is bound to one of the low-energy $n = 3$ clusters (**3a**, **3b**, and **3c**). They are less stable than **4a** by 1.5−3.6 kcal/mol. **4c** is a [0,4,2] structure where Na is surrounded by the four water molecules. This structure resembles the interior complex of neutral $Na(H_2O)_4$[25] with Na−O bonds but is less stable than **4a** by ∼2 kcal/mol. The Na−O surface structure **4g** is also less stable than **4a** by ∼4 kcal/mol.

As a summary, Na−H and hydrogen-bond interactions are important in dictating the structures of $[Na(H_2O)_n]^-$. In the most stable forms of $[Na(H_2O)_n]^-$ ($n = 1-4$), the water clusters interact with Na^- by H atoms by rearranging the hydrogen-bond network. The isomers with Na−O bonds are high-energy isomers for each *n*. Though **1b**, **2d**, **3e**, **4c**, and **4g** are similar to the neutral structures with the same *n*, they are not the most stable anion clusters for each *n*. Therefore, it is considered to be difficult to access the potential minima of the neutral complexes from the anion clusters by photoelectron spectroscopy for negatively charged $Na(H_2O)_n$ ($n = 1-4$).

3.2. Assignment and Size Dependence of PES Bands. In the photoelectron spectra (PES) of $[Na(H_2O)_n]^-$ by Takasu et al.,[16] the first and the second bands for the atomic Na anion appear at 0.55 and 2.65 eV, respectively. They are shifted to the higher electron binding energy (EBE) almost in parallel with each other by stepwise hydration. The amount of the shift in the vertical detachment energy (VDE) from the bare anion becomes as large as ca. 0.8 eV at $n = 4$.

The calculated VDEs of $[Na(H_2O)_n]^-$ for the transitions from the anionic ground state to the five lowest neutral states are listed in Table 1. They correspond to the transitions to the states derived from the atomic 3^2S, 3^2P, and 4^2S states in each cluster.

The VDE values for both 3^2S-3^1S and 3^2P-3^1S type transitions of atomic Na^- are calculated to be 0.53 and 2.59 eV, respectively, which agree with the observed first and second bands within 0.06 eV. For the 1:1 complex with Na−H interaction, **1a**, the calculated VDE for the 3^2S-3^1S-like transition is 0.77 eV and those for the 3^2P-3^1S-like transitions are 2.78−2.86 eV. They also coincide well with the experiment,

TABLE 1: Vertical Detachment Energies (eV) Corresponding to Transitions from Anionic Ground State to Ground and Low-Lying Excited States of Various Isomers of $[Na(H_2O)_n]^-$ ($n = 0-4$)[a] at the MRSDCI Level

$n = 0$			$n = 1$				
	calcd[b]			calcd			
expl	Na atom		expl	**1a**		**1b**	
0.55	3^2S	0.53	0.76	1^2A_1	0.77	$1^2A'$	0.43
2.65	3^2P	2.59	2.95	2^2A_1	2.78	$2^2A'$	1.94
				1^2B_1	2.80	$1^2A''$	2.00
				1^2B_2	2.86	$3^2A'$	2.20
	4^2S	3.67		3^2A_1	4.05	$4^2A'$	2.96

$n = 2$												
	calcd											
expl	**2a**		**2b**		**2c**		**2d**		**2e**		**2f**	
0.99	$1^2A'$	0.92	$1^2A'$	0.92	$1^2A'$	0.64	1^2A_1	0.43	1^2A	0.43	$1^2A'$	0.59
3.46	$2^2A'$	2.97	$2^2A'$	2.95	$2^2A'$	2.22	2^2A_1	1.48	2^2A	1.97	$2^2A'$	2.25
	$1^2A''$	3.00	$1^2A''$	2.99	$1^2A''$	2.34	1^2B_2	1.60	3^2A	2.05	$1^2A''$	2.27
	$3^2A'$	3.06	$3^2A'$	3.06	$3^2A'$	2.57	1^2B_1	1.85	4^2A	2.43	$3^2A'$	2.55
	$4^2A'$	4.35	$4^2A'$	4.32	$4^2A'$	3.44	3^2A_1	2.51	5^2A	2.99	$4^2A'$	3.41

$n = 3$										
	calcd									
expl	**3a**		**3b**		**3c**		**3d**		**3e**	
1.13	1^2A	1.13	1^2A_1	1.21	1^2A_1	1.02	1^2A_1	1.18	1^2A_1	0.34
3.49	2^2A	3.21	1^2B_2	3.35	1^2E	3.11	2^2A_1	3.27	1^2E	1.41
	3^2A	3.24	1^2B_1	3.38			1^2B_1	3.32		
	4^2A	3.29	2^2A_1	3.39	2^2A_1	3.16	1^2B_2	3.37	2^2A_1	1.42
	5^2A	4.64	3^2A_1	4.87	3^2A_1	4.53	3^2A_1	4.77	3^2A_1	2.21

$n = 4$														
	calcd													
expl	**4a**		**4b**		**4c**		**4d**		**4e**		**4f**		**4g**	
1.24	1^2A	1.10	$1^2A'$	1.39	1^2A	0.28	1^2A	1.23	$1^2A'$	1.33	$1^2A'$	1.44	1^2A	0.38
3.52	1^2E	3.16	$2^2A'$	3.55	2^2B	1.23	2^2A	3.34	$2^2A'$	3.46	$1^2A''$	3.64	1^2B	1.68
			$1^2A''$	3.58	1^2B	1.43	3^2A	3.37	$1^2A''$	3.48	$2^2A'$	3.67	2^2B	1.74
	2^2A	3.30	$3^2A'$	3.60	3^2A	1.56	4^2A	3.45	$3^2A'$	3.53	$3^2A'$	3.68	2^2A	2.14
	3^2A	4.64	$4^2A'$	5.12	4^2A	2.08	5^2A	4.90	$4^2A'$	4.96	$4^2A'$	5.27	3^2A	2.62

[a] Molecular structures are shown in Figures 1 and 2. [b] Only the **1s** orbital of Na was frozen in CI.

though the values for the excited states underestimate the experimental value slightly. For the isomer **1b** with Na−O bond, the lowest VDE is shifted to the lower EBE from $n = 0$, which is opposite to the experimental observation. The VDEs to the 3^2P-like states are below the observed second band by 0.75−1.01 eV. Thus, we can safely assign the first and the second PES bands to the transition to 3^2S- and 3^2P-like states in the most stable structure **1a**.

For $n = 2$, the lowest VDE for **2a** and **2b** is in good agreement with the first PES band. It is shifted to the blue from $n = 1$ by 0.15 eV. The calculated VDEs for the three low-lying excited states ($2^2A'$, $1^2A''$, and $3^2A'$) of **2a** and **2b** are also in reasonable agreement with the observed second band, though they underestimate the experimental value appreciably. On the other hand, the VDEs to the 3^2S-like state of other isomers (**2c**−**2f**) with Na−O bond(s) are shifted to the lower EBE from $n = 1$ and those for 3^2P-3^1S-like transitions are much lower than the VDE of the second PES band. Therefore, we have assigned the first and second PES bands to the transitions to 3^2S- and 3^2P-like states in the structures where one water molecule is bound to **1a** through hydrogen bond.

Among the $n = 3$ clusters, the structures **3a**−**3d** give similar VDEs to one another for both ground and excited states, but **3a** is considered to be responsible for the observed PES bands. Its lowest VDE agrees perfectly with the first band and those for the 3^2P-like transitions are close to the second band. On the other hand, the VDEs of **3e** with three Na−O bonds show different size dependence from other isomers, being shifted to the red from $n = 2$. We have assigned the PES bands to the most stable $n = 3$ cluster, **3a**.

The structures having Na−H and hydrogen-bond interactions for $n = 4$ (**4a**, **4b**, and **4d**−**4f**) also give the similar VDEs with one another and they are near the observed values, while those of the isomers with Na−O bonds (**4c** and **4g**) are much lower. This trend resembles the $n = 3$ clusters. Since it is known that such a small error around 0.4 eV can slip in the calculation in VDEs even at the high level calculation we employed, it is difficult to predict definitely which structure with Na−H and hydrogen bonds is responsible for the PES bands by only the calculated VDEs. Thus, we have tentatively assigned the PES bands to the cluster **4a** based on the energetics.

Here, we discuss the size dependence of the VDEs for $[Na(H_2O)_n]^-$ from the viewpoint of electronic state. In our previous paper, we showed that the blue shift of the first PES band with increasing n can be explained by the fact that the difference in the solvation energy between the anionic state and the neutral ground state at the most stable anionic structure becomes larger as n grows.

Shown in Table 2 are the expected values of the radial distribution (RD) for the unpaired electron of $Na(H_2O)_n$ at their anionic geometries calculated by having the Na atom at the origin. The RD values of the most stable hydrated clusters for each n are about 4.5 au for the ground state, 5.9−6.3 au for the 3^2P-like states, and 10.9−11.1 au for the 4^2S-like state. These

TABLE 2: Expected Values of Radial Distribution of Unpaired Electron (RD, au) for Neutral Ground and Low-Lying Excited States of $Na(H_2O)_n$ ($n = 0-4$) at Their Anionic Geometries[a]

$n = 0$		$n = 1$			
Na atom		**1a**		**1b**	
3^2S	4.486	1^2A_1	4.514	$1^2A'$	5.182
3^2P	6.459	2^2A_1	6.135	$2^2A'$	7.626
		1^2B_1	6.261	$1^2A''$	7.680
		1^2B_2	6.257	$3^2A'$	7.109
4^2S	11.492	3^2A_1	11.130	$4^2A'$	11.980

$n = 2$											
2a		**2b**		**2c**		**2d**		**2e**		**2f**	
$1^2A'$	4.492	$1^2A'$	4.493	$1^2A'$	4.965	1^2A_1	6.265	1^2A	5.135	$1^2A'$	5.015
$2^2A'$	6.019	$2^2A'$	6.043	$2^2A'$	6.889	2^2A_1	8.129	2^2A	7.059	$2^2A'$	6.990
$1^2A''$	6.129	$1^2A''$	6.158	$1^2A''$	6.665	1^2B_2	7.957	3^2A	7.167	$1^2A''$	6.768
$3^2A'$	6.154	$3^2A'$	6.173	$3^2A'$	7.114	1^2B_1	9.408	4^2A	8.312	$3^2A'$	7.517
$4^2A'$	11.088	$4^2A'$	11.128	$4^2A'$	11.754	3^2A_1	12.501	5^2A	11.900	$4^2A'$	11.721

$n = 3$									
3a		**3b**		**3c**		**3d**		**3e**	
1^2A	4.485	1^2A_1	4.453	1^2A_1	4.472	1^2A_1	4.476	1^2A_1	6.368
2^2A	5.983	1^2B_2	5.964	1^2E	6.052	2^2A_1	5.881	1^2E	9.217
3^2A	6.058	1^2B_1	5.919			1^2B_1	5.991		
4^2A	6.057	2^2A_1	5.831	2^2A_1	5.912	1^2B_2	6.038	2^2A_1	9.903
5^2A	10.922	3^2A_1	10.841	3^2A_1	11.107	3^2A_1	10.821	3^2A_1	12.773

$n = 4$													
4a		**4b**		**4c**		**4d**		**4e**		**4f**		**4g**	
1^2A	4.468	$1^2A'$	4.443	1^2A	8.041	1^2A	4.452	$1^2A'$	4.470	$1^2A'$	4.436	1^2A	5.507
1^2E	6.022	$2^2A'$	5.915	2^2B	9.727	2^2A	5.938	$2^2A'$	5.939	$1^2A''$	5.856	1^2B	7.602
		$1^2A''$	5.868	1^2B	10.728	3^2A	5.904	$1^2A''$	5.968	$2^2A'$	5.729	2^2B	8.080
2^2A	5.898	$3^2A'$	5.796	3^2A	10.130	4^2A	5.811	$3^2A'$	5.868	$3^2A'$	5.827	2^2A	9.302
3^2A	11.024	$4^2A'$	10.666	4^2A	13.418	5^2A	10.891	$4^2A'$	10.677	$4^2A'$	10.560	3^2A	12.233

[a] Geometries are given in Figures 1 and 2.

values do not change so much from those of the bare Na, even when n increases, which implies that the atomic nature of Na remains in the neutrals at these hydration structures. This trend is consistent with the fact that the VDEs of these clusters change by keeping their separation almost unchanged from the bare Na^-. On the other hand, when Na^- is hydrated from the O side, the RD values for both ground and excited states become larger rapidly with increasing number of Na−O bonds. As a result, the RDs for 3^2S- and 3^2P-like states in **4c** are more than 1.5 times as large as the corresponding atomic values. Therefore, the diffusion of the valence-electron distribution takes place in this type of hydration clusters in both ground and the lowest lying excited states. In the other words, the Na valence electron in these complexes is spread in the space on and between the ligating water molecules as n grows, giving rise to the one-center Rydberg-like state. The decrease in the energy separation between 3^2S- and 3^2P-like states with increasing n is considered to result from the change in the electronic nature from the atomic state to the diffuse Rydberg-like state.

In conclusion, both first and second PES bands for $[Na(H_2O)_n]^-$ ($n = 0-4$) are assignable to the most stable structure for each n with Na−H and hydrogen bonds. The atomic nature of Na is not affected very much in the neutrals for this hydration structure of Na^-, which is responsible for the blue shift of the second band nearly in parallel with the first band. It is interesting to notice that the size dependence of the VDEs for the isomers with maximum numbers of Na−O bonds is similar to that of $[Na(NH_3)_n]^-$.

3.3. Harmonic Frequencies and IR Spectra. In this section, we will investigate the harmonic frequencies and IR spectra of $[Na(H_2O)_n]^-$. It is well-known that the interplay between the ab initio MO calculations and the vibrational spectroscopy has been successful in studying the formation of the hydrogen bonds in the hydrated halogen anions.[52−56] As for the alkali atoms, the vibrational spectra have been reported only for the cationic state of Cs.[57] Though no experimental data for the hydrated alkali anions is available to date, it is expected to be instructive for the further study to predict the vibrational feature of hydration clusters of Na^- by ab initio MO calculations. In addition, the recent advance of the experimental technique IR-dip spectroscopy[58] enables us to obtain the vibrational information of the specific geometrical isomers. Thus, we discuss the IR spectra of $[Na(H_2O)_n]^-$ for the OH stretching region in relation to their structures, especially the hydrogen-bond network.

The calculated harmonic frequencies and IR intensities for the OH stretching vibrations of $[Na(H_2O)]^-$ and a water monomer are listed in Table 3. The numbers in the table are scaled by the average ratio between experimental[59] and calculated harmonic frequencies of the symmetric (ν_1) and antisymmetric (ν_3) OH stretching vibrations of a free water molecule (0.940), because the ab initio harmonic frequencies are known to overestimate the experimental values. The scaled theoretical frequencies of the ν_3 and ν_1 vibrations for the free H_2O are 3762 and 3650 cm^{-1}, respectively, and the former band is calculated to be more intense than the latter by about 5 times. In the most stable form of $[Na(H_2O)]^-$, **1a**, the ν_3 band is red-shifted from that of the free water by ca. 80 cm^{-1}, and the ν_1 band is by ∼50 cm^{-1}, respectively, while they both are shifted by ca. −160 cm^{-1} in the higher energy isomer, **1b**. The ν_1 band becomes much more intense than the ν_3 band in both 1:1 complexes, in sharp contrast to the free water monomer.

Next, we see the spectral change by further hydration, but focus only on the most stable structures for each n and selected

TABLE 3: Calulated Harmonic Frequencies (cm^{-1})[a] and IR Intensities (km/mol) of OH Stretching Vibrations for $[Na(H_2O)]^-$ and a Water Monomer Calculated by MP2 Method[b]

	1a[c]			**1b**[c]			H_2O		
no.	sym	freq	IR int	sym	freq	IR int	sym	freq[d]	IR int
1	B_2	3684	7.0	A″	3604	83.2	B_2	3762 (3756)	63.1
2	A_1	3599	393.2	A′	3489	856.6	A_1	3650 (3657)	13.4

[a] Scaled by 0.940. [b] All **1s** orbitals on heavy atoms were frozen in MP2 calculations. [c] Corresponds to structures in Figure 1. [d] Values in parenthese are by experiment (ref 59).

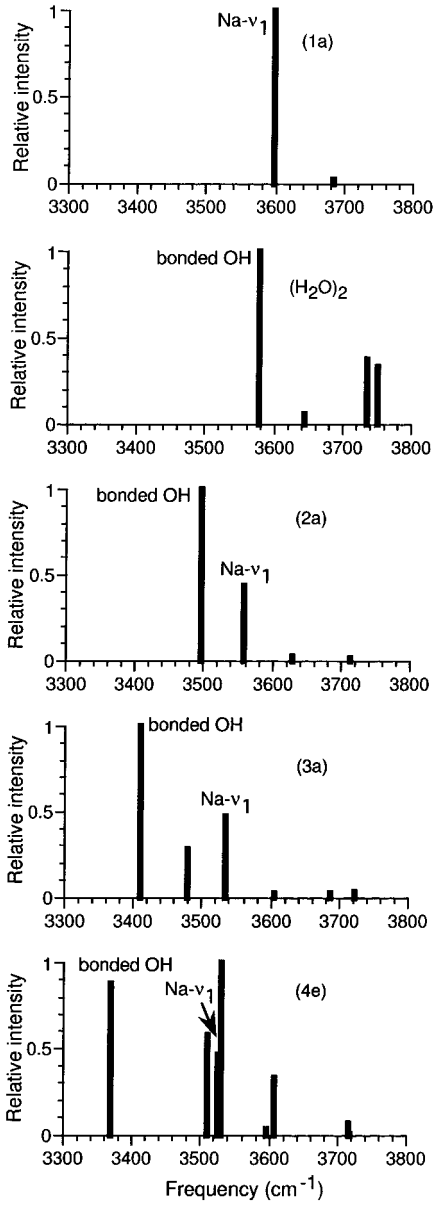

Figure 3. Calculated IR spectra of structures **1a**, **2a**, **3a**, and **4e** in Figures 1 and 2 and water dimer for OH stretch region.

isomers. Calculated frequencies and IR intensities for all structures in Figures 1 and 2 are tabulated in the Supporting Information (Tables IS−IVS).

At first, we examine the complexes **2a**, **3a**, and **4e**. The structure **2a** and **3a** are the most stable isomer for $n = 2$ and 3, respectively, while **4e** is one of the local minimum structures for $n = 4$. In **3a** and **4e**, the third and fourth water molecules are bound via hydrogen bonds to the oxygen atom in the proton-donor water in the water-dimer part of **2a**. The calculated IR spectra of these structures are shown in Figure 3 together with those of **1a** and the water dimer. Their normal modes of the OH stretching vibrations for each structure are given in the Supporting Information (Figure 2S). In pure $(H_2O)_2$, two bands have been observed experimentally at 3735 and 3601 cm^{-1}, which have been ascribed to the free OH and the hydrogen-bonded OH stretch.[60] In our calculation, the free OH band is at 3751 cm^{-1} for the proton-donor water and at 3735 cm^{-1} for the proton-acceptor part. On the other hand, the band for the hydrogen-bonded OH stretch, which we call the bonded OH band hereafter, is located at 3580 cm^{-1}, being more intense than the free OH bands.

For **2a**, the strongest band at 3498 cm^{-1} is also due to the hydrogen-bonded OH and it is red-shifted from the corresponding band of the pure water dimer by ~80 cm^{-1}. The normal mode of the second strongest band is mainly the symmetric OH stretch of the proton-acceptor water interacting directly with Na^-. Thus, we call this band the Na-ν_1 band for convenience. The frequency of this band (3558 cm^{-1}) is accidentally close to that of the bonded OH band of the water dimer. The free OH bands having higher frequencies are relatively weak, as is the case of **1a**. In the spectrum of **3a**, the bonded OH band is also the strongest and further shifted by ca. −90 cm^{-1} from **2a**. On the other hand, the frequency lowering of the Na-ν_1 band from **2a** is only ~20 cm^{-1} and its intensity relative to the bonded OH band is as large as that in **2a**. In addition, the new band appears between these two bands due to the newly formed hydrogen bond between **2a** and the third water molecule. The free OH bands are weak, as in **1a** and **2a**. For **4e**, we see that the bonded OH band keeps red-shifting, while the position of the Na-ν_1 band remains almost unchanged from **3a**. The other strong bands by the hydrogen-bonded OH of the third and fourth water molecules are almost overlapping with the Na-ν_1 band. Therefore, the rapid red-shift of the strong lowest band for the bonded OH, the gradual frequency lowering of the Na-ν_1 band, and the appearance of the bands at 3480−3530 cm^{-1} reflecting the numbers of water molecules bound to **2a** through hydrogen bonds are the distinctive feature in the IR spectra for these clusters. It is worth noticing that the amounts of the frequency lowering of the bonded OH band from the water dimer correlate roughly linearly with the elongations of the bonded OH distance in these clusters.[61]

Here, we mention briefly some low-energy isomers for $n =$ 3 and 4 (**3b**, **4b**, and **3d**) prior to the most stable, $[Na(H_2O)_4]^-$. Their IR spectra and normal modes are given in Supporting Information (Figures 4S and 5S). As for **3b**, four bands by the combinations of the ν_1 modes of two first-shell ligands and the ν_1 and ν_3 vibrations of the second-shell water are calculated at ca. 3560 −3630 cm^{-1}, and the symmetric OH stretch of the bridging water is the main contributor to the strongest band. In the spectrum of **4b**, the bands which can be attributed to the bonded and the free OH stretches of the water attached to **3b** appear in the lower and higher regions than the bands derived from **3b**. Their frequencies (3423 and 3723 cm^{-1}) are close to those of the corresponding bands of **3a**, and the bonded OH band is the most intense. On the other hand, the Na-ν_1 mode coupled with the in-phase stretches of two hydrogen-bonded OH shows the lowest frequency and the largest intensity for

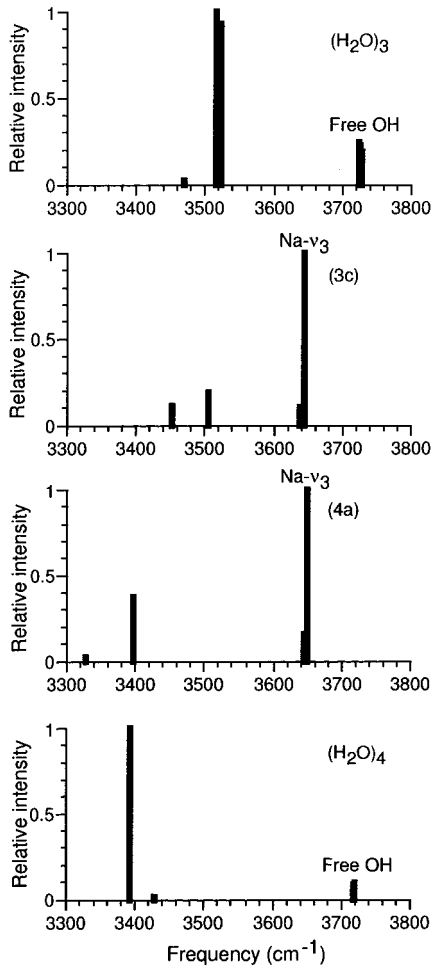

Figure 4. Calculated IR spectra of structures **3c** and **4a** in Figures 1 and 2, together with those of cyclic water trimer and tetramer for OH stretch region.

3d. The amounts of the red-shift of the Na-ν_1 band in **1a**, **2a**, and **3d** from the ν_1 band of the free water correlate almost linearly with the elongations of the OH bonds[61] interacting with Na^-, which resembles the bonded OH band for **1a**, **2a**, **3a**, and **4e**.

Now, we see the most stable $n = 4$ cluster, **4a**, and its analogue, **3c**. Their IR spectra together with those for cyclic $(H_2O)_3$ and $(H_2O)_4$ clusters are shown in Figure 4. Their normal modes are presented in the Supporting Information (Figure 3S). In contrast to the above-mentioned structures, the most intense band has high frequency around 3650 cm^{-1} for these pyramidal structures. The normal mode of the strongest band for **4a** shows that all OH bonds interacting with Na^- elongate and shorten in phase with one another. Two other bands due to OH bonds pointing to Na^- are close to this band, but they are relatively weak. We call these high-frequency bands the Na-ν_3 bands. On the other hand, the second strongest band due to the hydrogen-bonded OH stretch is at 3398 (**4a**) and 3507 (**3c**) cm^{-1}, and there is no band between the Na-ν_3 bands and this band. Therefore, we see the *window* region, which is as wide as 250 cm^{-1} for **4a**. This feature is similar to the cyclic water clusters, though the higher Na-ν_3 band is more intense than the lower hydrogen-bonded OH bands in the Na^-−water complex. The positions of the Na-ν_3 bands are shifted by ca. −80 cm^{-1} compared to the free OH bands of the pure water clusters.

Finally, we describe briefly the structures **1b**, **2d**, **3e**, and **4c**, whose electronic state has a diffuse Rydberg-like nature with increasing *n*. Their calculated IR spectra and normal modes of OH stretching vibrations are given in the Supporting Information (Figures 6S and 7S). From **1a** to **3e**, the IR bands can be divided into two groups. One is for the bands at ca. 3480−3530 cm^{-1}, including the strongest band for each structure, and another is for the weak bands at ca. 3590−3650 cm^{-1}. The former group can be attributed to the ν_1 vibrations of the water molecules and the latter to the ν_3 modes. In each spectrum, *n* bands in the ν_3 group almost overlap with one another and other *n* bands in the ν_1 group are also nearly degenerate. The quasidegeneracy of the bands in each group indicates that there is almost no hydrogen bond among water molecules. On the other hand, in the spectrum of **4c**, the ν_1 and the ν_3 groups are split into two subgroups, respectively. There are four pairs of bands reflecting the structure. Two lowest pairs with large intensities are by the ν_1 vibrations, while the other pairs of the high-frequency bands are by the ν_3 vibrations. Though the spectrum of **4c** becomes slightly complicated due to the weak water−water interactions, the near constancy of the lowest and the strongest ν_1 band against *n* is characteristic of these complexes.

4. Concluding Remarks

In the present paper, we have studied the geometries, VDEs, and IR spectra of $[Na(H_2O)_n]^-$ ($n = 1-4$) by an ab initio MO method at a correlated level with the extended basis sets. The conclusions we have reached are as follows.

(1) The most stable 1:1 complex has the symmetric C_{2v} form in which the water molecule is bound to Na^- from the H side. In the larger clusters, the hydrogen bonds among water molecules as well as the Na−H interaction become important in dictating the structures. The pyramidal complex in which each molecule in the cyclic water cluster points one OH bond to Na^- and another OH to the neighboring water becomes the most stable at $n = 4$. The structures with as many Na−O bonds as possible are high-energy isomers for all *n* examined. The minimum-energy structures of $[Na(H_2O)_n]^-$ differ from those of the neutrals with the same *n*, and thus it is difficult to access the potential minima of the neutral complexes from the anionic clusters by the photoelectron spectroscopy.

(2) The calculated VDEs for the most stable structures for each *n* are in good agreement with the experiment. All observed PES bands can be assigned to the $3^2S(Na)-3^1S(Na^-)$ and $3^2P(Na)-3^1S(Na^-)$ type transitions perturbed by the hydration. They are shifted to the higher EBE with increasing *n* by keeping the separation between the first and the second bands almost unchanged. On the other hand, for the isomers with Na−O bonds, the VDEs of the transition to the neutral ground state decreases slightly and those of the transitions to the 3^2P-like states become smaller rapidly as *n* grows, which is similar to the experimental observation for $[Na(NH_3)_n]^-$.

(3) The atomic character remains in the electronic state of the neutrals at the most stable geometries of $[Na(H_2O)_n]^-$. This feature is responsible for the near constancy of the difference in the VDEs between the first and the second PES bands. In contrast, the isomers with the maximum numbers of Na−O bonds take on the diffuse one-center Rydberg-like state with stepwise hydration. This change in the electronic nature results in the rapid decrease of the separation in VDEs between the transition to the ground state and those to the low-lying excited states.

(4) In the IR spectrum of the most stable $[Na(H_2O)]^-$, the ν_1 band of the water becomes much more intense than the ν_3 band, which is in remarkable contrast to the isolated water monomer. For the most stable $[Na(H_2O)_2]^-$, the strong band appears in the lower region rather than in the above Na-ν_1 band, indicating

the formation of the hydrogen bond between water molecules. This band is red-shifted in the spectrum of the most stable $[Na(H_2O)_3]^-$, reflecting the elongation of the bonded OH. On the other hand, for the most stable $[Na(H_2O)_4]^-$, the strongest band at around 3650 cm^{-1} is due to the stretching vibrations of the OH bonds interacting directly with Na^-. The hydrogen-bonded OH bands are relatively weak and located at around 3400 cm^{-1}. The window region between the Na-ν_3 bands and the hydrogen-bonded OH bands is characteristics for the pyramidal structure.

Acknowledgment. We thank Prof. Fuke and Dr. Takasu (Kobe University) for their valuable discussions. This work was financially supported in part by the Grant-in-Aid from the Ministry of Education, Science, Sports and Culture of Japan. Support from Japan Science and Technology Corporation (JST) is also acknowledged. A part of computations was carried out at the Computer Center at the Institute for Molecular Science. We are grateful for the allotment of computer time at IMS.

Supporting Information Available: A figure of optimized geometries of high-energy isomers of $[[Na(H_2O)_3]^-$ (Figure 1S); two figures of normal modes for OH stretching vibrations of **1a**, **2a**, **3a**, and **4e** (Figure 2S) and those of **3c** and **4a** (Figure 3S); four figures of calculated IR spectra and normal modes for OH stretch region of structures that we do not discuss in detail in text (Figures 4S−9S); and tables of all calculated frequencies of structures in Figures 1 and 2 (Tables IS−IVS). This information is available free of charge via the Internet at http://pubs.acs.org.

References and Notes

(1) Dogonadze, R. R.; Kalman E.; Kamyshev, A. A.; Ulstrup, J., Eds. *Solvation Phenomena in Specific Physical, Chemical, and Biological Systems (The chemical physics of solvation, Part C)*; Elsevier: Amsterdam, 1988.

(2) Schulz, C. P.; Haugstatter, R.; Tittes, H. U.; Hertel, I. V. *Phys. Rev. Lett*. **1986**, *57*, 1703.

(3) Schulz, C. P.; Haugstatter, R.; Tittes, H. U.; Hertel, I. V. *Z. Phys. D* **1988**, *10*, 279.

(4) Hertel, I. V.; Huglin, C.; Nitsch, C.; Schulz, C. P. *Phys. Rev. Lett.* **1991**, *67*, 1767.

(5) Nitsch, C.; Schulz, C. P.; Gerber, A.; Zimmermann-Edling, W.; Hertel, I. V. *Z. Phys. D* **1992**, *22*, 651.

(6) Schulz, C. P.; Hohndorf, J.; Brockhaus, P.; Hertel, I. V. *Z. Phys. D* **1997**, *40*, 78.

(7) Nitsch, C.; Huglin, C.; Hertel, I. V.; Schulz, C. P. *J. Chem. Phys.* **1994**, *101*, 6559.

(8) Schulz, C. P.; Hohndorf, J.; Brockhaus, P.; Noak, F.; Hertel, I. V. *Chem. Phys. Lett.* **1995**, *239*, 18.

(9) Schulz, C. P.; Nitsch , C. *J. Chem. Phys.* **1997**, *107*, 9794.

(10) Brockhaus, P.; Hertel, I. V.; Shultz, C. P. *J. Chem. Phys.* **1999**, *110*, 393.

(11) Rodham, D. A.; Blake G. A. *Chem. Phys. Lett.* **1997**, *264*, 522.

(12) Wang K.; Rodham, D. A.; Mckoy V.; Blake G. A. *J. Chem. Phys.* **1998**,*108*, 4817.

(13) Misaizu, F.; Tsukamoto, K.; Sanekata, M.; Fuke, K. *Chem. Phys. Lett.* **1992**, *188*, 241.

(14) Misaizu, F.; Fuke, K.; Hashimoto, K. In *Structures and dynamics of clusters*; Kondow, T.; Kaya, K.; Terasaki, A., Eds.; Universal Academy Press: Tokyo, 1996; pp 383.

(15) Takasu, R.; Hashimoto, K.; Fuke, K. *Chem. Phys. Lett.* **1996**, *258*, 94.

(16) Takasu, R.; Misaizu, F.; Hashimoto, K.; Fuke, K. *J. Phys. Chem. A* **1997**, *101*, 3078.

(17) Takasu, R.; Taguchi, T.; Hashimoto, K.; Fuke, K. *Chem. Phys. Lett.* **1998**, *290*, 481.

(18) Greer, J. C.; Huglin, C.; Hertel, I. V.; Ahlrichs, R. *Z. Phys. D* **1994**, *30*, 69.

(19) Barnett, R. N.; Landman, U. *Phys. Rev. Lett.* **1993**, *70*, 177.

(20) Makov, G.; Nitzan A. *J. Phys. Chem.* **1994**, *98*, 3549.

(21) Stampfli, P.; Bennemann, K. H. *Comput. Matter. Sci.* **1994,** *2*, 578.

(22) Stampfli, P. *Phys. Rep.* **1995**, *255*, 1.

(23) Hashimoto, K.; He, S.; Morokuma, K. *Chem. Phys. Lett.* **1993**, *206*, 297.

(24) Hashimoto, K.; Morokuma, K. *Chem. Phys. Lett.* **1994**, *223*, 423.

(25) Hashimoto, K.; Morokuma, K. *J. Am. Chem. Soc.* **1994**, *116*, 11436.

(26) Hashimoto, K.; Morokuma, K. *J. Am. Chem. Soc.* **1995**, *117*, 4151.

(27) Hashimoto, K.; Kamimoto, T. *J. Am. Chem. Soc.* **1998**, *120*, 3560.

(28) Hashimoto, K.; Kamimoto, T.; Fuke, K. *Chem. Phys. Lett.* **1997**, *266*, 7.

(29) McLean, A. D.; Chandler, G. S. *J. Chem. Phys.* **1980**, *72*, 5639.

(30) Hehre, W. J.; Radom, L.; Schleyer, P. v. R.; Pople, J. A. *Ab initio molecular orbital theory*; Wiley: New York, 1986.

(31) Strey, G. *J. Mol. Spectrosc*. **1967**, *24*, 87.

(32) Werner, H.-J.; Knowles, P. J. *J. Chem. Phys.* **1985**, *82*, 5053.

(33) Knowles, P. J.; Werner, H.-J. *Chem. Phys. Lett.* **1985**, *115*, 259.

(34) Werner, H.-J.; Knowles, P. J. *J. Chem. Phys.* **1988**, *89*, 5803.

(35) Knowles, P. J.; Werner, H.-J. *Chem. Phys. Lett.* **1988**, *145*, 514.

(36) Knowles, P. J.; Werner, H.-J. *Theor. Chim. Acta* **1992**, *84*, 95.

(37) (a) Frisch, M. J.; Trucks, G. W.; Head-Gordon, M.; Gill, P.; Wong, M. W.; Foresman, J. B.; Johnson, B. G.; Schlegel, H. B.; Robb, M. A.; Replogle, E. S.; Gomperts, R.; Andres, J. L.; Raghavachari, K.; Binkley, J. S.; Gonzalez, C.; Martin, R. L.; Fox, D. J.; DeFrees, D. J.; Baker, J.; Stewart, J. P.; Pople, J. A. *Gaussian 92*, Gaussian Inc., Pittsburgh, PA, 1992. (b) Frisch, M. J.; Trucks, G. W.; Schlegel, H. B.; Gill, P. M. W.; Johnson, B. G.; Robb, M. A.; Cheeseman, J. R.; Keith, T.; Petersson, G. A.; Montgomery, J. A.; Raghavachari, K.; Al-Laham, M. A.; Zakrzewski, V. G.; Ortiz, J. V.; Foresman, J. B.; Cioslowski, J.; Stefanov, B. B.; Nanayakkara, A.; Challacombe, M.; Peng, C. Y.; Ayala, P. Y.; Chen, W.; Wong, M. W.; Andres, J. L.; Replogle, E. S.; Gomperts, R.; Martin, R. L.; Fox, D. J.; Binkley, J. S.; Defrees, D. J.; Baker, J.; Stewart, J. P.; Head-Gordon, M.; Gonzalez, C.; Pople. A. *Gaussian 94*, Gaussian, Inc., Pittsburgh, PA, 1995.

(38) MOLPRO is a package of ab initio programs written by H.-J. Werner and P. J. Knowles, with contributions of J. Almlof, R. D. Amos, M. J. O. Deegan, S. T. Elbert, C. Hampel, W. Meyer, K. Peterson, R. Pitzer, A. J. Stone, P. R. Taylor, R. Lindh, M. E. Mura, and T. Thorsteinsson.

(39) Kisrenmacher, H.; Popkie H.; Clementi E. *J. Chem. Phys.* **1973**, *58*, 5627.

(40) Kisrenmacher, H.; Popkie H.; Clementi E. *J. Chem. Phys.* **1973**, *59* 5842.

(41) Hiraoka, K.; Mizuse S.; Yamabe, S., *J. Phys. Chem.* **1988**, *92*, 3943.

(42) Zhan, C.-C.; Iwata, S. *Chem. Phys. Lett.* **1995,** *232*, 72.

(43) Combariza, J. E.; Kestner, N. R. *J. Phys. Chem.* **1994**, *98*, 3513.

(44) Xantheas, S. S.; Dunning, T. H., Jr. *J. Phys. Chem.* **1994**, *98*, 1348.

(45) Xantheas, S. S.; Dang, L. X., *J. Phys. Chem.* **1996**, *100*, 3989.

(46) Xantheas, S S, *J. Phys. Chem.* **1996**, *100*, 9703.

(47) Combariza, J. E.; Kestner, N. R.; Jortner, J. *J. Chem. Phys.* **1994**, *100*, 2851.

(48) Curtiss, L. A.; Frurip, D. L.; Blander, M. *J. Chem. Phys.* **1979,** *71*, 2703.

(49) Xantheas, S. S.; Dunning, T. H., Jr. *J. Chem. Phys.* **1993**, *99*, 8774.

(50) Combariza, J. E.; Kestner, N. R.; Jortner, J. *Chem. Phys. Lett.* **1993,** *203*, 423.

(51) Combariza, J. E.; Kestner, N. R.; Jortner, J. *Chem. Phys. Lett.* **1994**, *221*, 156.

(52) Cabarcos, O. M.; Weinheimer, C. J.; Lisy, J. M.; Xantheas, S. S. *J. Chem. Phys.* **1999,** *110*, 5.

(53) Choi, J-H.; Kuwata, K. T.; Cao, Y-B.; Okumura, M. *J. Phys. Chem. A* **1998**, *102*, 503.

(54) Ayotte, P.; Bailey, C. G.; Weddle, G. H.; Johnson, M. A., *J. Phys. Chem. A* **1998**, 102, 3067.

(55) Johnson, M. S.; Kuwata, K. T.; Wong, C-K.; Okumura, M, *Chem. Phys. Lett.* **1996**, *260*, 551.

(56) Bailey, C. G.; Kim. J.; Dessent, C. E. H.; Johnson, M. A. *Chem. Phys. Lett.* **1997**, *269*, 122.

(57) Weinheimer C. J.; Lisy J. M. *J. Chem. Phys.* **1996**, *105*, 2938.

(58) Ebata, T. In *Nonlinear Spectroscopy for Molecular Structure Determination*; Field, R. W., Hirota, E., Maier, J. P., Tsuchiya, S., Eds.; Blackwell Science: Oxford, 1998; Chapter 6.

(59) Benedict, W. S.; Gailar, N.; Plyler, K. *J. Chem. Phys.* **1956**, *24*, 1139.

(60) Huisken F.; Kaloudis M.; Kulcke A. *J. Chem. Phys*. **1996**, *104*, 17.

(61) OH distance of a free water monomer and bonded OH length in a water dimer are calculated to be 0.960 and 0.965 Å, respectively.